

ChemComm

Accepted Manuscript



This is an *Accepted Manuscript*, which has been through the Royal Society of Chemistry peer review process and has been accepted for publication.

Accepted Manuscripts are published online shortly after acceptance, before technical editing, formatting and proof reading. Using this free service, authors can make their results available to the community, in citable form, before we publish the edited article. We will replace this *Accepted Manuscript* with the edited and formatted *Advance Article* as soon as it is available.

You can find more information about *Accepted Manuscripts* in the [Information for Authors](#).

Please note that technical editing may introduce minor changes to the text and/or graphics, which may alter content. The journal's standard [Terms & Conditions](#) and the [Ethical guidelines](#) still apply. In no event shall the Royal Society of Chemistry be held responsible for any errors or omissions in this *Accepted Manuscript* or any consequences arising from the use of any information it contains.

Cite this: DOI: 10.1039/c0xx00000x

www.rsc.org/xxxxxx

ARTICLE TYPE

Charge state-dependent catalytic activity of $[\text{Au}_{25}(\text{SC}_{12}\text{H}_{25})_{18}]$ nanoclusters for the two-electron reduction of dioxygen to hydrogen peroxide

Yizhong Lu,^{a,b} Yuanyuan Jiang,^{a,b} Xiaohui Gao^{a,b} and Wei Chen^{a*}

Received (in XXX, XXX) Xth XXXXXXXXXX 20XX, Accepted Xth XXXXXXXXXX 20XX
DOI: 10.1039/b000000x

The electrochemical production of H_2O_2 from O_2 catalyzed by $[\text{Au}_{25}(\text{SC}_{12}\text{H}_{25})_{18}]$ was studied as a function of the charge states (-1, 0 and +1). Maximum H_2O_2 production (~90%) was obtained from the negatively charged clusters (Au_{25}^-) due to the efficient electron transfer from the anionic Au_{25}^- cluster into the LUMO (π^*) of O_2 .

As a promising sustainable energy carrier, hydrogen peroxide (H_2O_2), have been one of the most important chemicals in the world and produced in large scale in industry. The oxygen reduction reaction (ORR) in aqueous solutions occurs mainly by two pathways: the direct 4-electron reduction pathway from O_2 to H_2O , and the 2-electron reduction pathway from O_2 to H_2O_2 . In polymer electrolyte membrane fuel cells (PEMFCs), the 4-electron direct pathway is highly preferred. In contrast, the 2-electron reduction pathway is then used in industry for H_2O_2 production. These two pathways always compete with each other during the ORR process. Such situation in turn presents the hope of finding an active, selective, and stable electrocatalyst for the production of H_2O_2 from oxygen *via* a two-electron reduction process.

Recently, gold nanoclusters, which consist of only several to tens of metal atoms, exhibited promising applications in catalysis.¹ Of particular interest is $\text{Au}_{25}(\text{SR})_{18}$ cluster whose structure has been well characterized by theoretical calculations² and single-crystal X-ray crystallography.³ Previous theoretical and experimental studies have revealed that anionic Au nanoclusters can activate the O_2 molecule and generate superoxo- or peroxy-like *via* electron transfer from the Au nanoclusters core to the LUMO (π^*) of the O_2 molecule.⁴ Recently, extensive studies have demonstrated that the anionic charge of atomically precise Au_{25}^- nanoclusters could facilitate the adsorption and activation of molecular species, such as O_2 and CO_2 ,^{4b,5} and thus improve the reactivity of the clusters.⁶ Inspired by these interesting findings, here, for the first time, we studied the electrocatalytic activity of $[\text{Au}_{25}(\text{SC}_{12}\text{H}_{25})_{18}]$ nanoclusters for the synthesis of H_2O_2 from two-electron reduction of dioxygen and investigated the influence of the cluster charge states on the electrochemical production of H_2O_2 in alkaline media.

Atomically precise Au_{25} nanoclusters with different charge states (-1, 0 and +1) were synthesized through an efficient one-phase method (see Electronic Supplementary Information).

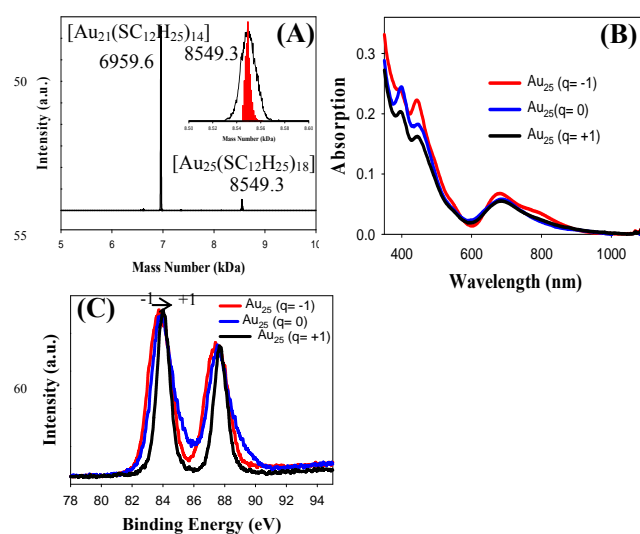


Fig. 1 (A) MALDI-TOF mass spectra of Au_{25}^- nanoclusters dissolved in N_2 -saturated CH_2Cl_2 solution. Inset shows the zoom-in spectra in the range of mass number 8.50-8.60 kDa. The red patterns are from theoretical simulation. (B) UV-Vis absorption spectra of Au_{25}^- (red curve); Au_{25}^0 (blue curve); and Au_{25}^+ (black curve). (C) XPS spectra of Au_{25} nanoclusters with different charge states, Au_{25}^- (red curve); Au_{25}^0 (blue curve); Au_{25}^+ (black curve).

It should be pointed out that in the previous reports, Au_{25} nanoclusters were usually produced at 0°C with very low stirring speed during the synthesis. In the present revised approach, by adding TOAB (1.2 eq to HAuCl_4) and changing the HAuCl_4 concentration (10 mM) and the ratio of RSH to HAuCl_4 (5:1), anionic Au_{25}^- nanoclusters can be synthesized at room temperature without any limit of stirring speed. The composition, monodispersity and purity of the as-synthesized clusters were first analyzed by MALDI-TOF MS under very low laser pulse intensity (just above the threshold intensity). As shown in Fig. 1A, a clean MALDI spectrum was obtained with an intense peak at ~8549.3 Da, which can be assigned to the intact $[\text{Au}_{25}(\text{SC}_{12}\text{H}_{25})_{18}]^-$ ion (theoretical value: 8549.61 Da). The experimental MS profile agrees well with the simulated isotopic patterns (Fig. 1A inset). Note that due to the laser-induced fragmentation, a peak at ~6959.6 Da assigned to $[\text{Au}_{21}(\text{SC}_{12}\text{H}_{25})_{14}]$ was also observed.⁷ In the UV-Vis spectra (Fig. 1B), there are three distinct absorption

bands centered at 677, 443, and 392 nm For the Au₂₅⁻ nanoclusters, which are the characteristic spectroscopic fingerprints of the thiol-capped Au₂₅⁻ nanoclusters.^{3b,8} Apart from the three main absorption bands, there are additional fine spectral features, including a broad shoulder at ~800 nm, and another small shoulder at ~550 nm. To our surprise, the present revised synthesis can enhance the yield of Au₂₅⁻ nanoclusters to ca. 60% by Au atom. Note that the reported highest yield of [Au₂₅(SR)₁₈]⁻ TOA⁺ was 49%.⁸ From the UV-Vis spectra shown in Fig. S1, the UV-Vis absorption of the crude product is almost superimposable with that of the purified nanoclusters, indicating an extraordinarily high purity of the as-synthesized Au₂₅⁻ nanoclusters. Both UV-Vis absorption and MS analysis unambiguously demonstrate the successful synthesis of Au₂₅⁻ nanoclusters with high purity and yield.

Due to their highly sensitive to the local environment, anionic Au₂₅⁻ nanoclusters could be easily converted to charge neutral Au₂₅⁰ nanoclusters by bubbling the CH₂Cl₂ solution with O₂.⁹ Earlier studies have shown that the charge state of the Au₂₅ nanoclusters could be conveniently identified from their optical spectroscopic features, that is, the relative intensities of the 400 and 450 nm peaks as well as the presence or absence of the 800 nm shoulder peak.⁸⁻⁹ One could clearly see from Fig. 1B that, for the neutral charge Au₂₅⁰ nanoclusters, the absorption peak at 400 nm becomes more prominent while the 450 nm peak becomes less so compared to that of the Au₂₅⁻ clusters. Concurrently, the 800 nm shoulder that is the characteristic of Au₂₅⁻ nanoclusters disappears and a new, small shoulder at 630 nm emerges. These results indicate the successful conversion of charge negative Au₂₅⁻ nanoclusters to charge neutral Au₂₅⁰, which is similar to the earlier reports.⁸⁻⁹ Meanwhile, according to the previous reports, the cationic Au₂₅⁺ nanoclusters can be produced by using strong oxidizing agent, such as Ce(SO₄)₂.¹⁰ It can be seen from Fig. 1B that the spectroscopic fingerprints of Au₂₅⁰ and Au₂₅⁺ are different from the original Au₂₅⁻ clusters.¹¹ In addition, XPS are also used to distinguish the Au₂₅ nanoclusters with different charge states. As shown in Fig. 1C, the Au 4f_{7/2} binding energy (BE) of the gold clusters shows a positive shift with the charge states changing from -1 (83.74 eV), 0 (83.89 eV), to +1 (84.02 eV), further suggesting the successful synthesis of Au₂₅ nanoclusters with different charge states.¹²

The reduction of dioxygen to hydrogen peroxide was investigated in 0.1 M KOH solution using a GC RRDE with the same loading of the three kinds of gold clusters (20 μg/cm²). The H₂O₂ production could be easily evaluated from the RRDE currents at a fixed potential (0.5 V vs. SCE), where the oxygen reduction current is negligible and H₂O₂ oxidation is diffusion-limited. Compared to the CV in N₂-saturated electrolyte, obvious reduction current can be observed from the oxygen reduction catalyzed by the gold clusters (Fig. 2A). However, based on the current density and onset potential, the charge state of the Au₂₅ shows significant effect on their catalytic activity. The most positive onset potential and the largest current density of ORR were obtained from the negatively charged clusters, indicating the highest catalytic activity of Au₂₅⁻ clusters for ORR. Compared to the large Au nanoparticles (Au NPs, ~11 nm, TEM and UV-Vis spectrum are shown in Fig. S2 and S3), the Au₂₅ nanoclusters exhibited enhanced ORR catalytic activity. Fig. 2B shows the

RRDE voltammograms recorded at GC blank electrode and the Au₂₅ nanoclusters. Similar to the CV results, the Au₂₅⁻ (-0.115) shows more positive onset potential than Au₂₅⁰ (-0.15 V) and Au₂₅⁺ (-0.18 V) nanoclusters. Moreover, the half-wave potential on Au₂₅⁻ nanoclusters is -0.3 V, about 20 and 50 mV more positive than those at the Au₂₅⁰ and Au₂₅⁺. These results indicate that within the present experimental context, the electrocatalytic activity of Au₂₅ nanoclusters for O₂ reduction to H₂O₂ increases with the decrease of the charge states, with Au₂₅⁻ nanoclusters showing the highest activity.

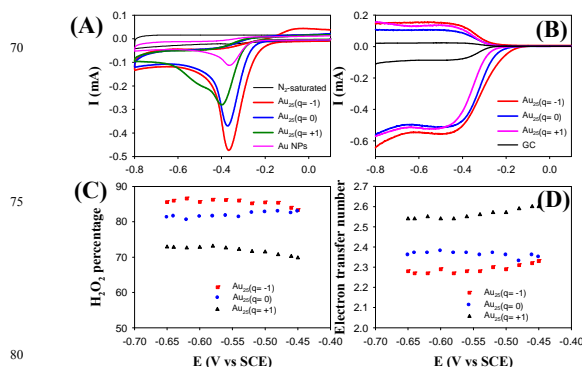


Fig. 2 (A) CVs of ORR on Au NPs and the Au₂₅ nanoclusters with different charge states in 0.1 M KOH saturated with oxygen and N₂ (Au₂₅⁻, black curve). Potential scan rate 0.1 V/s. (B) RRDE voltammograms recorded on GC electrode and the Au₂₅ nanoclusters (with loading of 20 μg/cm²) with different charge states in O₂-saturated 0.1 M KOH solution at 1600 rpm rotation rate. The disk potential was scanned at 10 mV/s and the ring potential was constant at 0.5 V. (C) Percentage (or selectivity) of H₂O₂ and (D) the electron transfer number (n) of Au₂₅ nanoclusters as a function of the applied potentials, based on the RRDE data in B.

The electron transfer number (n) and the percentage of hydrogen peroxide produced at the different Au₂₅ clusters can be evaluated from the RRDE measurements based on the following equations¹³

$$H_2O_2\% = 200 \times \frac{i_r / N}{i_D + i_r / N} \quad (1)$$

$$n = 4 \times \frac{i_D}{i_D + i_r / N} \quad (2)$$

where i_D is the disk current, i_r is the ring current, and N is the current collection efficiency of the Pt ring (0.37).

As shown in Fig. 2C, the H₂O₂ production percentages on Au₂₅⁰ and Au₂₅⁺ clusters are 72% and 82%, respectively, which increases up to 86% on Au₂₅⁻ clusters. The corresponding electron transfer number was calculated to be 2.28, 2.35, and 2.56, respectively, on Au₂₅⁻, Au₂₅⁰, and Au₂₅⁺. The above results indicate that dominant two-electron ORR process occurs on Au₂₅ nanoclusters and Au₂₅⁻ could be used as a promising electrocatalyst for the electrochemical synthesis of H₂O₂ in alkaline media. It should be noted that compared to the present [Au₂₅(SC₁₂H₂₅)₁₈], the Au₂₅ nanoclusters passivated by short-chain ligands, phenylethylthiol, are favourable for the oxygen reduction to H₂O₂.^{1a} Therefore, the protecting ligands covered on the cluster surface can also affect the catalytic properties. As can be seen from Fig. S4A, the diffusion-limiting currents at -0.5 V on Pt/C (1.12 mA) is nearly 2 times that of the Au₂₅⁻ (0.55 mA), further indicating the dominant 2e ORR process on Au₂₅⁻. Moreover, from Fig. S4B, only 2.1% H₂O₂ production

percentages was obtained on Pt/C over the potential range of -0.65 to -0.45 V, and the calculated electron transfer number is 3.96. The above electrochemical results show that Pt/C is a kind of good catalyst for 4-electron reduction of dioxygen to water, and Au₂₅⁻ nanoclusters, however, are excellent catalysts for production of peroxide from 2 electron reduction of dioxygen.

Further investigations on the electrocatalytic synthesis of H₂O₂ at the different charged gold clusters have also been performed by RDE measurements. Fig. S5 shows the ORR polarization curves at different rotation speeds with current normalized by the geometrical area of electrodes. According to the Levich equation,^{1a} the slopes of the plots for Au₂₅⁻, Au₂₅⁰, and Au₂₅⁺ are -0.077, -0.054, -0.071 mA/cm² rpm, respectively (Fig. S6), which agrees well with the theoretical value for the two-electron transfer process (-0.0714 mA/cm² rpm).

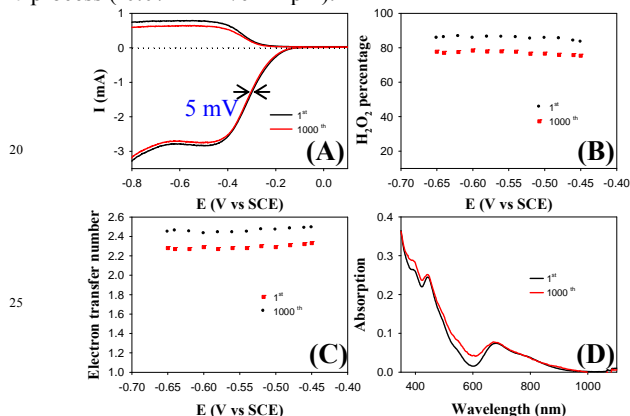


Fig. 3. Durability tests of Au₂₅⁻ nanoclusters by performing accelerated durability tests (ADTs) for 1000 cycles. (A) RRDE voltammograms in O₂-saturated 0.1 M KOH solution, with a scan rate of 10 mV/s and 1600 rpm rotation rate. (B) Percentage (or selectivity) of H₂O₂ and (C) The electron transfer number (n) of Au₂₅⁻ nanoclusters as a function of the applied potentials, based on the RRDE data in A. (D) UV-Vis spectra of Au₂₅⁻ nanoclusters before and after 1000 cycles of ADTs tests.

To examine the stability of the Au₂₅⁻ nanoclusters, accelerated durability tests (ADTs) were performed in O₂-saturated 0.1 M KOH solution by applying a cyclic potential sweep between -0.60 and 0.00 V. As can be seen from Fig. 3A, after 1000 cycles, the half-wave potential of negative charged Au₂₅⁻ nanoclusters show only a 5 mV negative shift. Moreover, the H₂O₂ percentage decreases only about 9% (Fig. 3B), while the electron transfer number increase from ~2.28 to ~2.45 (Fig. 3C) after the durability tests. Besides, UV-Vis measurements (Fig. 3D) show that the Au₂₅⁻ nanoclusters retain the characteristic absorption features after the ADTs. These results strongly indicate that negatively charged Au₂₅ clusters show high stability and high selectivity for the two-electron reduction of dioxygen to hydrogen peroxide.

Mechanistically, oxygen adsorption and subsequently activation on the catalyst surface is the first step in the electroreduction of oxygen. Generally, activation of O₂ molecules on the bulk gold surface is thermodynamically unfavorable for the formation of chemisorbed intermediate.^{4b} While for Au₂₅ nanoclusters, the much lower coordination number of the surface atoms and the unique electronic structure (electron-rich icosahedral Au₁₃ core surrounded by electron-deficient 12 Au atoms) render them more active for electrocatalytic oxygen reduction.^{1a} In addition, DFT

calculations have suggested that charging a cluster can increase its chemical activity with respect to oxygen.^{4b} On the basis of earlier experimental and theoretical calculations,^{4a, 5, 14} we propose that the strong effect of charge states on the electrocatalytic production of H₂O₂ could be attributed to the electron transfer from the anionic Au₂₅ cores into the LUMO (π^*) of O₂, which can activate the O₂ molecule and generate peroxo-like species.

In summary, we present a study of electrocatalytic synthesis of H₂O₂ in alkaline media by Au₂₅ clusters and the effect of cluster charge states on their catalytic activity. The electrochemical studies showed that the maximum H₂O₂ production and the most efficient 2e dioxygen reduction were obtained from the charge negative Au₂₅⁻ nanoclusters, followed by the neutral and cationic ones, indicating the significant effect of charge states of Au₂₅ cluster on its catalytic properties. The present study has provided an insight into the highly selective two-electron reduction of dioxygen to hydrogen peroxide by controlling the charge states of gold nanoclusters.

This work was supported by the National Natural Science Foundation of China (No. 21275136).

Notes and references

^a State Key Laboratory of Electroanalytical Chemistry, Changchun Institute of Applied Chemistry, Chinese Academy of Sciences, Changchun 130022, Jilin, China. Tel: +86431-85262061; E-mail:

weichen@ciac.ac.cn

^b University of Chinese Academy of Sciences, Beijing 100039, China

† Electronic Supplementary Information (ESI) available: Detailed experimental procedures, additional structural characterizations and electrochemical measurements. See DOI: 10.1039/b000000x/

- (a) W. Chen and S. W. Chen, *Angew. Chem. Int. Edit.*, 2009, 48, 4386; (b) Y. Z. Lu and W. Chen, *Chemical Society Reviews*, 2012, 41, 3594; (c) R. C. Jin, *Nanoscale*, 2010, 2, 343; (d) Y. Yu, Q. F. Yao, Z. T. Luo, X. Yuan, J. Y. Lee and J. P. Xie, *Nanoscale*, 2013, 5, 4606; (e) M. A. H. Muhammed and T. Pradeep, *Small*, 2011, 7, 204.
- J. Akola, M. Walter, R. L. Whetten, H. Hakkinen and H. Gronbeck, *J. Am. Chem. Soc.*, 2008, 130, 3756.
- (a) M. W. Heaven, A. Dass, P. S. White, K. M. Holt and R. W. Murray, *J. Am. Chem. Soc.*, 2008, 130, 3754; (b) M. Zhu, C. M. Aikens, F. J. Hollander, G. C. Schatz and R. Jin, *J. Am. Chem. Soc.*, 2008, 130, 5883.
- (a) H. Tsunoyama, N. Ichikuni, H. Sakurai and T. Tsukuda, *J. Am. Chem. Soc.*, 2009, 131, 7086; (b) G. Mills, M. S. Gordon and H. Metiu, *J. Chem. Phys.*, 2003, 118, 4198.
- D. R. Kauffman, D. Alfonso, C. Matranga, H. F. Qian and R. C. Jin, *J. Am. Chem. Soc.*, 2012, 134, 10237.
- Y. Zhu, H. F. Qian, B. A. Drake and R. C. Jin, *Angew. Chem. Int. Edit.*, 2010, 49, 1295.
- A. Dass, A. Stevenson, G. R. Dubay, J. B. Tracy and R. W. Murray, *J. Am. Chem. Soc.*, 2008, 130, 5940.
- J. F. Parker, J. E. F. Weaver, F. McCallum, C. A. Fields-Zinna and R. W. Murray, *Langmuir*, 2010, 26, 13650.
- (a) M. Z. Zhu, W. T. Eckenhoff, T. Pintauer and R. C. Jin, *J. Phys. Chem. C*, 2008, 112, 14221; (b) A. C. Dharmaratne, T. Krick and A. Dass, *J. Am. Chem. Soc.*, 2009, 131, 13604.
- (a) Y. Negishi, N. K. Chaki, Y. Shichibu, R. L. Whetten and T. Tsukuda, *J. Am. Chem. Soc.*, 2007, 129, 11322; (b) J. P. Choi and R. W. Murray, *J. Am. Chem. Soc.*, 2006, 128, 10496.
- M. Z. Zhu, G. R. Chan, H. F. Qian and R. C. Jin, *Nanoscale*, 2011, 3, 1703.
- C. Zhou, C. Sun, M. X. Yu, Y. P. Qin, J. G. Wang, M. Kim and J. Zheng, *J. Phys. Chem. C*, 2010, 114, 7727.

-
- 13 Y. Y. Liang, Y. G. Li, H. L. Wang, J. G. Zhou, J. Wang, T. Regier
and H. J. Dai, *Nat. Mater.*, 2011, 10, 780.
- 14 (a) M. Okumura, Y. Kitagawa, T. Kawakami and M. Haruta, *Chem.*
Phys. Lett., 2008, 459, 133; (b) Y. Z. Lu and W. Chen, *J. Power*
5 *Sources*, 2012, 197, 107.